ARTICLE

Check for updates

cFLIP$_S$ regulates alternative NLRP3 inflammasome activation in human monocytes

Yuhui Gao [1,2,7], Shi Yu [2,6,7], Mengdan Chen[2], Xun Wang[3], Lei Pan[2,4], Bin Wei [1✉] and Guangxun Meng [2,4,5✉]

The innate immune responses, including inflammasome activation, are paramount for host defense against pathogen infection. In contrast to canonical and noncanonical inflammasome activation, in this study, heat-killed gram-negative bacteria (HK bacteria) were identified as single-step stimulators of the NLRP3 inflammasome in human monocytes, and they caused a moderate amount of IL-1β to be released from cells. Time course experiments showed that this alternative inflammasome response was finished within a few hours. Further analysis showed that the intrinsically limited NLRP3 inflammasome activation response was due to the negative regulation of caspase-8 by the short isoform of cFLIP (cFLIPs), which was activated by NF-κB. In contrast, overexpressed cFLIP$_S$, but not overexpressed cFLIP$_L$, inhibited the activation of caspase-8 and the release of IL-1β in response to HK bacteria infection in human monocytes. Furthermore, we demonstrated that TAK1 activity mediated the expression of cFLIPs and was upstream and essential for the caspase-8 cleavage induced by HK bacteria in human monocytes. The functional specificity of cFLIPs and TAK1 revealed unique responses of human monocytes to a noninvasive pathogen, providing novel insights into an alternative regulatory pathway of NLRP3 inflammasome activation.

INTRODUCTION

The innate immune system plays a key role in host defense against infections. Upon microbial challenge, the recognition of pathogen-associated molecular patterns (PAMPs) by pattern recognition receptors (PRRs) is the first step in initiating human innate immune responses. Some PRRs also recognize endogenous danger-associated molecular patterns (DAMPs) and initiate inflammatory responses [1, 2]. NOD-like receptor (NLR) family pyrin domain-containing 3 (NLRP3) is an important PRR with a three-domain structure, which includes a carboxy-terminal leucine-rich repeat (LRR) domain, a central nucleotide binding domain with ATPase activity (NACHT), and an amino-terminal pyrin domain (PYD) that recruits apoptosis-related spot-like proteins containing CARD (ASC) for inflammasome assembly [3]. Recruited ASCs undergo oligomerization, which promotes the autoprocessing of caspase-1 and drives the maturation and release of proinflammatory cytokines such as interleukin-1β (IL-1β) and IL-18 [4, 5]. Concomitant caspase-1 activation leads to proteolysis of the pore-forming protein gasdermin D (GSDMD) [6], which enables the secretion of IL-1β and causes pyroptotic cell death [7].

The activation of the NLRP3 inflammasome has been classified into three pathways. In the canonical and noncanonical pathways, the triggering signal is often mediated by microbial components or endogenous cytokines that stimulate the transcriptional and posttranslational priming of NLRP3 and pro-IL-1β [8]; then, an extracellular signal is transmitted from pore-forming toxins, ATP, particulate matter, or intracellular recognition of lipopolysaccharide (LPS) to caspase-4/5 and caspase-11, which activate the NLRP3 inflammasome [9, 10]. Canonical and noncanonical inflammasome activation often result in cleavage of many caspase-1 molecules, the release of IL-1β and pyroptotic cell death mediated by cleaved GSDMD [6, 11, 12]. In contrast, human monocytes are characterized by an alternative inflammasome pathway that is triggered by extracellular LPS sensed by Toll-like receptor 4 (TLR4) and initiates NLRP3 inflammasome activation through a single signal mediated via the FADD-CASP8-RIPK1 axis [13]. In addition to LPS, apolipoprotein C3 has been reported to activate an alternative NLRP3 inflammasome pathway [14]. Compared to the robustness of canonical and noncanonical NLRP3 inflammasome activation, the activation of alternative inflammasome activation is weak, marked by mild release of low levels of IL-1β and an undetectable cell death rate [15]. In addition, a high concentration of extracellular K^+ does not inhibit the activation of the alternative NLRP3 inflammasome activation pathway.

Although LPS has been used as an agonist to study the alternative inflammasome activation pathway in humans, whether

[1]School of Life Sciences, Shanghai University, Shanghai 200444, China. [2]The Center for Microbes, Development and Health, CAS Key Laboratory of Molecular Virology & Immunology, University of Chinese Academy of Sciences, Shanghai 200031, China. [3]Shanghai Blood Center, Shanghai 200051, China. [4]Pasteurien College, Soochow University, Suzhou 215006 Jiangsu, China. [5]Nanjing Advanced Academy of Life and Health, Nanjing 211135 Jiangsu, China. [6]Present address: Department of Basic Research, Guangzhou Laboratory, Guangzhou International Bio-Island, Guangzhou 510005 Guangdong, China. [7]These authors contributed equally: Yuhui Gao, Shi Yu. ✉email: weibinwhy@shu.edu.cn; gxmeng@ips.ac.cn

live-attenuated bacteria trigger the same pathway to mount a mild inflammatory response is unclear. Live-attenuated gram-negative bacteria function as complete particles and, therefore, compared to soluble LPS, are more physiologically relevant. In addition, it is unclear how human innate immune cells respond to noninvasive gram-negative bacteria in the environment to inhibit cell death as well as local inflammation. Moreover, although physiological inflammation is essential for protective immunity, uncontrolled inflammation may lead to tissue destruction and autoinflammatory or autoimmune diseases [16, 17]. In recent years, the molecular mechanisms that negatively regulate canonical and noncanonical inflammasome activation have been extensively studied [18–20]. However, little is known about the negative regulatory mechanisms or limiting factors that inhibit alternative inflammasome pathway activation in human monocytes.

In the present work, we utilized heat-killed gram-negative bacteria to stimulate human monocytes and studied the alternative activation of the NLRP3 inflammasome pathway. We found that these bacteria stimulated the release of only a moderate level of IL-1β and the death of a negligible number of cells. Through temporal experiments, we found that mild inflammasome activation resulted from the negative regulation of caspase-8 activation. We demonstrated that the short isoform of cell FLICE (FADD-like IL-1β converting enzyme) inhibitory protein (cFLIP$_S$) exerted a regulatory effect on caspase-8 activation, thus inhibiting the activation of the NLRP3 inflammasome in human monocytes. Moreover, we found that TAK1 was an upstream molecule of caspase-8 and thus was involved in the alternative activation of inflammasomes, as well as in the expression of cFLIP$_S$. These data provide important insights into the negative alternative regulation of the NLRP3 inflammasome in human cells.

MATERIALS AND METHODS
Cell lines and reagents
THP-1 monocytes (CAT #TIB-202; American Type Culture Collection [ATCC]) were maintained in RPMI 1640 (Gibco) with 10% FBS (FBSSA500-S; AusGeneX), 1% penicillin/streptomycin (15140-122; Life Technologies), and 50 μM β-ME at 37 °C with 5% CO$_2$. Human primary blood mononuclear cells (PBMCs) were isolated from the peripheral blood of healthy donors (Shanghai Blood Center). Briefly, fresh human PBMCs were separated using Ficoll-Paque PLUS (10302181; Cytiva) and SepMate 50 mL centrifugation tubes (STEMCELL Technologies) at $1200 \times g$ for 10 min at room temperature (RT). PBMCs were washed three times with filtered PBS containing 0.5% FBS and 2 mM EDTA at $500 \times g$ for 5 min. PBMCs were counted and resuspended in RPMI 1640 medium supplemented with 1% FBS and 1% streptomycin/penicillin, and the cell concentration in the resuspension was 10×10^6 cells/ml (with monocytes accounting for approximately 20% of all cells). HEK293T (catalog no. CRL-3216; ATCC) cells were maintained in DMEM (SH30243.02; HyClone) with 10% FBS and 1% penicillin/streptomycin. Mycoplasma contamination was monitored by PCR throughout the project.

Bacterial culture and heat inactivation
E. coli XL10 (XL10-Gold, CAT #200314, Stratagene), enteropathogenic *E. coli* (EPEC) E2348/69 (kindly provided by Dr. Feng Shao) and *Salmonella Typhimurium* (*S. typhimurium*) SL1344 (generously shared by Dr. Hong Tang) were maintained in Luria–Bertani medium (10 g tryptone, 5 g yeast extract, 10 g NaCl in 1 L ddH$_2$O, pH 7.4). Solid medium was supplemented with 1.5% agar powder. The culture concentration was determined by spectrophotometry (OD$_{600}$). Cells were centrifuged at 3500 rpm for 5 min, washed three times and suspended to the appropriate density in sterile PBS. Bacteria were heat-inactivated by incubation at 75 °C for 30 min. Complete inactivation was confirmed by plating the suspensions on solid medium and incubating them at 37 °C for 24 h.

Reagents and antibodies
MCC950 (PZ0280; Sigma–Aldrich), 5Z-7-oxozeaenol (O9890; Sigma–Aldrich), nigericin (tlrl-nig; Invitrogen), propidium iodide (P4864; Sigma–Aldrich), Hoechst 33342 (T5840; TargetMOI), Z-IETD-FMK (HY-101297; MCE), cycloheximide (239763-5GM-M; Sigma–Aldrich), raptinal (1176-09-6; AdipoGen), LPS from *E. coli* O111:B4 (S1732; Beyotime), poly(dA:dT) (tlrl-patrh; InvivoGen), BV6 (HY-16701, MCE), Z-VAD-FMK (HY-16658B, MCE), recombinant human TNF-α (300-01A; PeproTech), TPCA1 (HY-10074, MCE), and BAY 11-7082 (HY-13453, MCE). The following antibodies were used for immunoblotting: rabbit anti human caspase-1 (3866, Cell Signaling Technology), goat anti-human IL-1β (AF-201-NA; R&D Systems), mouse anti-human NLRP3 Cryo-2 (AG-20B-0014-C100; Adipogen), rabbit anti-TAK1 (4505; Cell Signaling Technology), mouse anti -β-actin (10021787; Proteintech), rabbit anti-P-TAK1 (4508 s; Cell Signaling Technology), rabbit anti-GSDMD (A18281; ABclonal), mouse anti-caspase-8 (9746 s; Cell Signaling Technology), rabbit anti-human GAPDH (2118; Cell Signaling Technology), mouse anti-cFLIP (sc-5276; Santa Cruz Biotechnology), rabbit anti-cleaved caspase-3 (9661 s, Cell Signaling Technology), mouse anti-His-Tag (AE003; ABclonal), rabbit anti-DDDDK-Tag (AE092; ABclonal), rabbit anti-TRIF (4596 s, Cell Signaling Technology), and rabbit anti-NF-κB p65 (8242 s, Cell Signaling Technology).

Inflammasome stimulation
THP-1 monocytes were seeded at 2×10^5 cells/well in FBS-free RPMI 1640 medium in 96-well plates (Thermo), treated with heat-killed *E. coli* XL10 (4 $\times 10^5$ bacteria/well), heat-killed EPEC (4 $\times 10^5$ bacteria/well), heat-killed S. typhimurium (4 $\times 10^5$ bacteria/well), raptinal (1 μg/ml), or LPS and incubated at 37 °C with 5% CO$_2$. Cell pretreatment with inhibitors MCC950 (10 μM), Z-IETD-FMK (25 μM), 5Z-7-oxozeaenol (1 μM), TPCA-1 (1 μM), BAY 11-7082 (2 μM) or cycloheximide (1 μg/ml) for 0.5 h or with KCL (30 mM) for 10 min. PBMCs were seeded at 10×10^6 cells/well in 1% FBS RPMI 1640 medium in 96-well plates. Inhibitor pretreatment and stimulation were the same as described above. The lysate sample used for immunoblotting was a full-well lysate, and the supernatant samples were derived from additional replicates. To show that heat-killed bacteria-treated PBMCs and THP-1 monocytes are responsive to further inflammasome stimulation, cells were treated without or with 10 μM nigericin for an additional 1 hour before the supernatants and cell lysates were collected. To induce AIM2 inflammasome activation, 2 μg poly(dA:dT) was added to 96-well plates and stimulated for 6 h. To induce necroptosis, cells were pretreated with BV6 (1 μM) and Z-VAD-FMK (25 μM) for 1 h and stimulated with recombinant human TNF-α (50 ng/ml) (TBZ) for 14 h.

Live/dead staining assay
For PI and Hoechst 33342 dead–live staining, THP-1 monocytes were seeded at 5×10^4 cells/well in FBS-free RPMI 1640 medium containing propidium iodide (PI, 5 μg/ml) and Hoechst 33342 (500 ng/ml). Inhibitor pretreatment and stimulation were the same as described above. Fluorescence images were taken with an Olympus FV-1200 microscope. The ratio of PI to Hoechst 33342 cells per field of view (FOV) was quantified and analyzed by ImageJ software.

Enzyme-linked immunosorbent assay (ELISA)
The amount of mature IL-1β released in the cell culture supernatant was measured and analyzed using an IL-1β ELISA kit (IL-1β, DY201; R&D Systems) according to the manufacturer's instructions. Absorbance was measured at wavelengths of 450 nm and 570 nm. The absorbance obtained at 450 nm wavelength minus the absorbance obtained at 570 nm wavelength was the true absorbance of a sample well. The data points are displayed in bar charts as the mean ± S.E.M. Final concentrations were plotted against plate standards. Concentration results are shown as pg/ml.

CRISPR/Cas9-mediated gene targeting
Gene-deficient THP-1 cells were generated using CRISPR/Cas9-mediated gene targeting technology. Briefly, LentiCRISPR v2 (#52961; Addgene) containing sgRNA specifically targeting the indicated genes was packaged in HEK293T cells. The sgRNA sequences targeted the following genes: human *NLRP3* (GAAGAAGACGTACACCGCGG), human *MAP3K7* or TAK1 (GATCGACTACAAGGAGATCG), human *CFLAR* (GGGCCGAGGCAAGA TAAGCA), human *RELA* (AGACGATCGTCACCGGATTG), and human *TICAM1* (AGTCCGAAACACCGTCAATG). Lentiviral particles were produced in HEK293T cells by cotransfection with an LentiCRISPR v2-sg plasmid, PSPAX2, and VSV-glycoprotein at a 4:3:2 ratio using Lipofectamine 2000 (11668019; Thermo Fisher Scientific). The lentiviral particles in the supernatants were centrifuged and used to infect THP-1 monocytes. One

day post-infection, the cells were subjected to puromycin selection at a concentration of 2 μg/ml for 72 h. Surviving cells were subjected to limiting dilution and seeded in 96-well plates to obtain stable single clones deficient in the respective genes.

cFLIP overexpression in THP-1 cells
For the generation of the cFLIP-overexpressing THP-1 cell line, a lentiviral vector containing the 2x flag-tagged human cFLIP gene was constructed. The cloning primer sequences for targeting following respective genes were cFLIP$_L$, 5′-AAGCCTGCACTAGCGTTAACGATGTCTGCTGAAGTCATCCAT-CAGG-3′ (forward) and 5′-TTATCGATAAGCTTGATATCGTTATGTGTAGGAGA GGATAAG-3′ (reverse), and cFLIP$_S$, 5′-AAGCCTGCACTAGCGTTAACGATGTCT GCTGAAGTCATCCATCAGG-3′ (forward) and 5′-TTATCGATAAGCTTG ATATC GTTAATCACATGGAACAATTTCCAAGAATT-3′ (reverse). The cloned products and plasmids were ligated with an EasyGeno Single Assembly Cloning kit (VI202; TIANGEN) according to the manufacturer's instructions. Lentiviral particles were generated in 293T cells by transfection with fugw-2 x flag-cFLIP, PSPAX2, and VSV-glycoprotein at a 5:4:1 ratio using Lipofectamine 2000 and harvested 48 h later for use in infecting THP-1 monocytes. Cells were seeded in 96-well plates to obtain single clones stably over-expressing the respective genes. The efficiency of overexpression was confirmed using western blots. To insert cFLIP$_S$ back into the *CFLAR* knockout cell lines, the cFLIP$_S$-encoding gene was mutated; the GGCCGAGGCAAGATAAGC sequence was changed to GGACGCG-GAAAAATCAGT. The cells were subjected to G418 selection at a concentration of 400 μg/ml.

Real-time PCR
THP-1 cell RNA was extracted by TRIzol Reagent (15596018; Thermo Fisher Scientific) and reverse transcribed into cDNA using a GoSript™ Reverse Transcription kit (Promega). Real-time PCR was performed using SYBR Green Real-time PCR Master Mix (TOYOBO) on an ABI QuantStudio 6 flex Real-time PCR System (Thermo Fisher Scientific). The relative expression levels of target genes were normalized to the level of GAPDH via the formula [2$^{-\Delta Ct(target\ gene-GAPDH)}$] and reported as a relative unit (RU). The following primers were used: for cFLIP$_L$, 5′- ATAACTTCAGGCTCCATAATGG-GAGAAG-3′ (forward) and 5′-GCTCTGTCTCATTGCCAATGCAATC-3′ (reverse) and for cFLIP$_S$, 5′- TGGAGAAACTAAATCTGGTTGCCCC-3′ (forward) and 5′-TTCAGATCAGGACAATGGGCATAGG -3′ (reverse).

Immunoprecipitation
HEK293T cells were transfected with 400 ng fugw-2 x flag-cFLIP$_S$ and 200 ng PCDN4-caspase-8(C360A)-His in 24-well plates (Thermo). Forty-eight h post-transfection, the cells were treated with lysis buffer (0.5% NP40; 145 mM NaCl; 25 mM Tris; 5% glycerol, pH 7.3; and 1x protease inhibitor cocktail) for 30 min at 4 °C and centrifuged at 16,000 × *g* for 15 min, and the supernatant was incubated with anti-DDDDK-Tag antibody-conjugated Protein G agarose beads (37478 S; Cell Signaling Technology). The samples were washed five times in immunoprecipitation lysis buffer, and the protein complexes were eluted with 2x loading buffer at 95 °C for 15 min. To construct the overexpressed caspase-8 plasmid, the cloning primer sequences used for targeting the respective gene were 5′-TTGGTACCGAGCTCGATGGACTTCAGCAGAAATC-3′ (forward) and 5′-TGATGGTGATGATGAGCATCAGAAGGGAAGACAAG-3′ (reverse), and muta-genesis was performed to generate C360A.

Statistical analyses
Data analyses were performed with GraphPad Prism software version 8.0.2. Bar graphs are presented as the mean values ± SEMs. The results with multiple groups were analyzed using one-way ANOVA. The p values are as follows: ns, not significant; *$p < 0.05$; **$p < 0.01$; ***$p < 0.001$; ****$p < 0.0001$.

RESULTS
Heat-killed gram-negative bacteria induce mild NLRP3 inflammasome activation in a single step in human monocytes
To investigate alternative NLRP3 inflammasome activation path-ways in human monocytes, we used undifferentiated THP-1 monocytic cells as previously described [21], and examined mature IL-1β release and caspase-1 cleavage after challenge with gram-negative bacteria for 6 h at twice the number over monocytes. Although live *E. coli* induced the release of high levels of mature

IL-1β release into the cell culture supernatant, several forms of live-attenuated (including heat-killed, antibiotic suppression and UV radiation) *E. coli* stimulated the cells in the absence of a second signaling event, leading to moderate levels of IL-1β secreted (Supplementary Fig. 1A). Using clustered regularly interspaced short palindromic repeats (CRISPR)-guided knockout of relevant genes in THP-1 cells, we found that the loss of NLRP3 inhibited caspase-1 cleavage and mature IL-1β release after gram-negative bacterial challenge (Supplementary Fig. 1B, C). Moreover, we also detected the cleavage rate of the pore-forming protein GSDMD carboxyl-terminus (C-terminus) in a NLRP3-dependent manner (Supplemen-tary Fig. 1B, C). Notably, the activation of the NLRP3 inflammasome induced by heat-killed *E. coli* was enhanced with an increase in the number of heat-killed bacteria (Supplementary Fig. 1D).

In addition to those of *E. coli* XL10, the effects of heat-killed (HK) EPEC (enteropathogenic *Escherichia coli*) and *S. typhimurium* (*Salmonella typhimurium*) were evaluated on human peripheral blood multinuclear cells (PBMCs) isolated from healthy donors. Similar to their effects on THP-1 monocytic cells, heat-killed EPEC and *S. typhimurium* induced inflammasome activation and the release of mature IL-1β in PBMCs after 16 h of stimulation, and these cells were found to be sensitive to inhibition by the NLRP3-specific inhibitor MCC950 (10 μM) (Fig. 1A–D). Notably, after treating monocytes with heat-killed gram-negative bacteria, we detected a minimal cell death rate, as revealed by ratios of propidium iodide (PI)-stained nuclei (dead cells) and Hoechst 33342-stained nuclei (live cells); these results were NLRP3-dependent (Fig. 1E, F).

To better characterize the inflammasome / cell death pathways for which activation was limited, we used nigericin, a canonical NLRP3 inflammasome agonist, to treat HK-bacteria-treated cells. Notably, the addition of 10 μM nigericin to HK-bacteria-treated cells greatly enhanced the maturation and release rate of IL-1β within 1 hour (Supplementary Fig. 2A–D). In addition, compared to the that after heat-killed bacteria treatment alone, the cell death rate was significantly increased after nigericin stimulation (Supplementary Fig. 2E, F). These results demonstrated that the activation of the NLRP3 inflammasome mediated by heat-killed gram-negative bacteria resulted in minimal rates of cell death and that the treated cells retained the capacity to respond to further challenge to mediate pyroptotic inflammasome activation.

Caspase-8 activity is involved in heat-killed gram-negative bacterium-induced NLRP3 inflammasome activation
The alternative NLRP3 inflammasome pathway activation stimu-lated by LPS is mediated by factors such as TRIF, FADD, caspase-8 and RIPK1 [13]. In our experiment, treatment with heat-killed gram-negative bacteria induced the cleavage of pro-caspase-8 in THP-1 monocytes (Fig. 2A). In addition, the activation of caspase-8 and caspase-1 was significantly inhibited by 25 μM Z-IETD-FMK (Fig. 2B), suggesting that caspase-8 cleavage occurred upstream of caspase-1 activation. Moreover, in human PBMCs, we found that Z-IETD-FMK significantly inhibited the activation of caspase-1 and the release of IL-1β in cells after stimulation by heat-killed gram-negative bacteria (Fig. 2C, D). Using CRISPR-guided knockout of *TICAM1* in THP-1 cells, we found that the loss of TRIF inhibited caspase-8 cleavage and NLRP3 inflammasome activation induced by heat-killed gram-negative bacteria (Supplementary Fig. 3A–D).

Potassium efflux is an important trigger for canonical and noncanonical inflammasome activation [22, 23]. Moreover, the nigericin- and ATP-activated NLRP3 canonical inflammasome and intracytoplasmic LPS-mediated caspase-4/5 activation (of the noncanonical inflammasome) can were inhibited by high con-centrations of extracellular K$^+$. In our experiments, treatment with a high concentration (30 mM) of extracellular K$^+$ led to a significant inhibitory effect on the activation of caspase-1 and the release of IL-1β induced by nigericin (Fig. 2E, F); in contrast, as expected, treatment with a high concentration of extracellular K$^+$ did not inhibit the caspase-1 activation induced by heat-killed
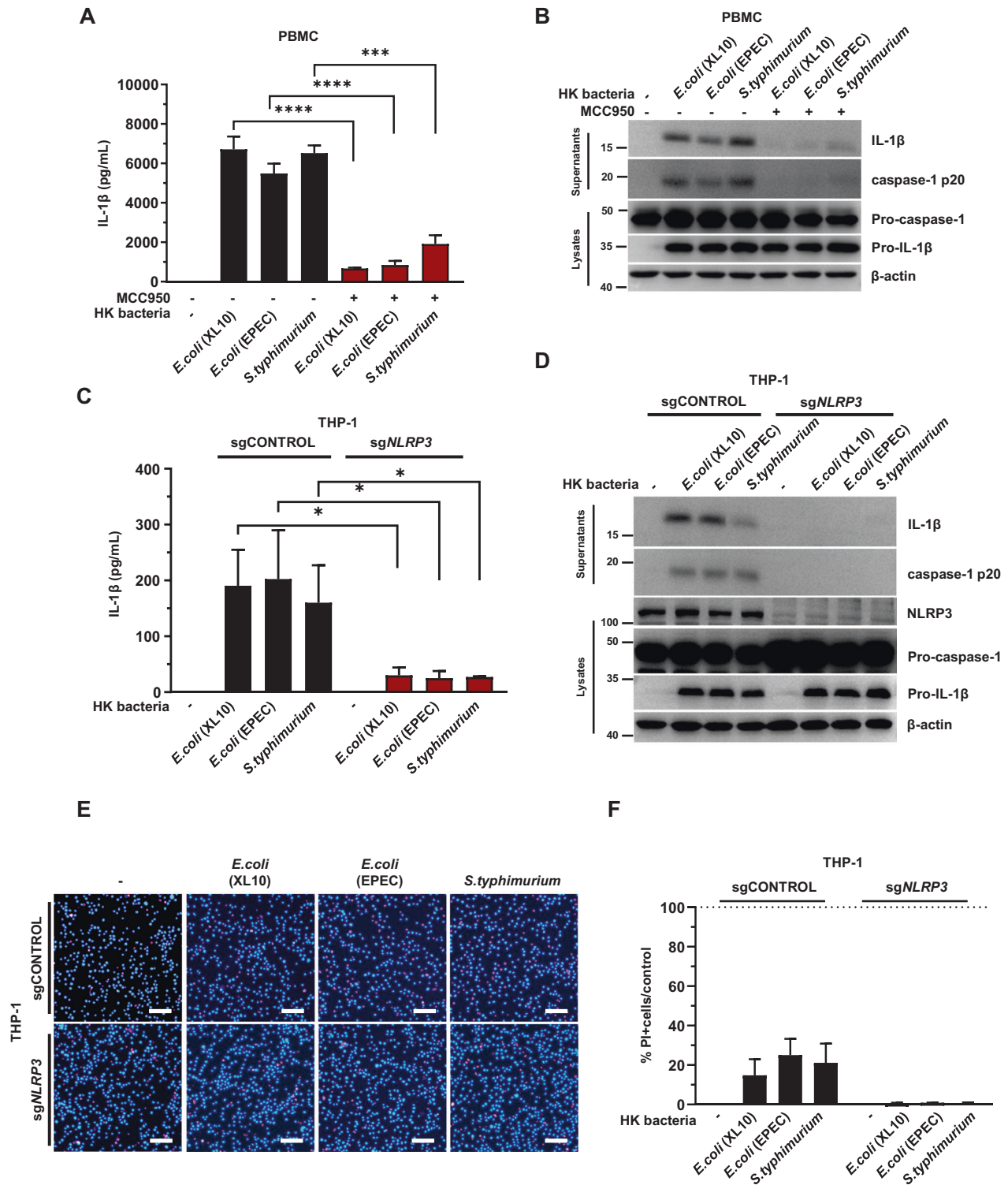
Fig. 1 NLRP3 inflammasome activation is induced in human monocytes by heat-killed gram-negative bacteria. **A**, **B** PBMCs were untreated or were pretreated for 0.5 h with MCC950 (10 μM) and stimulated for 16 h with heat-killed gram-negative bacteria at twice the number of the monocytes, as indicated. **A** IL-1β secretion in the cell culture supernatant is representative of the mean ± SEM from one of two donors. One-way ANOVA was performed to determine statistical significance. ***$p < 0.001$; ****$p < 0.0001$. **B** Immunoblots showing IL-1β and caspase-1 in the cell culture supernatant and total cell lysates as shown in **A**. **C**, **D** Control and *NLRP3*-KO THP-1 monocytes were stimulated for 6 h with heat-killed gram-negative bacteria. **C** IL-1β secretion in the cell culture supernatant is shown as the mean ± SEM. One-way ANOVA was performed to determine statistical significance. *$p < 0.05$. **D** Immunoblots showing NLRP3, IL-1β and caspase-1 in the cell culture supernatant and total cell lysate are representative of one of two experimental repeats. **E**, **F** Fluorescence microscopy of THP-1 monocytes after stimulation for 6 h with heat-killed gram-negative bacteria in twice the number of cells. **E** Representative images of cells stained with PI (red) and Hoechst (blue) are representative of one of two experimental repeats. Scale bars denote 100 μm. **F** The number of PI-positive cells shown in **E** was counted with ImageJ. Error bars show the means ± SEMs
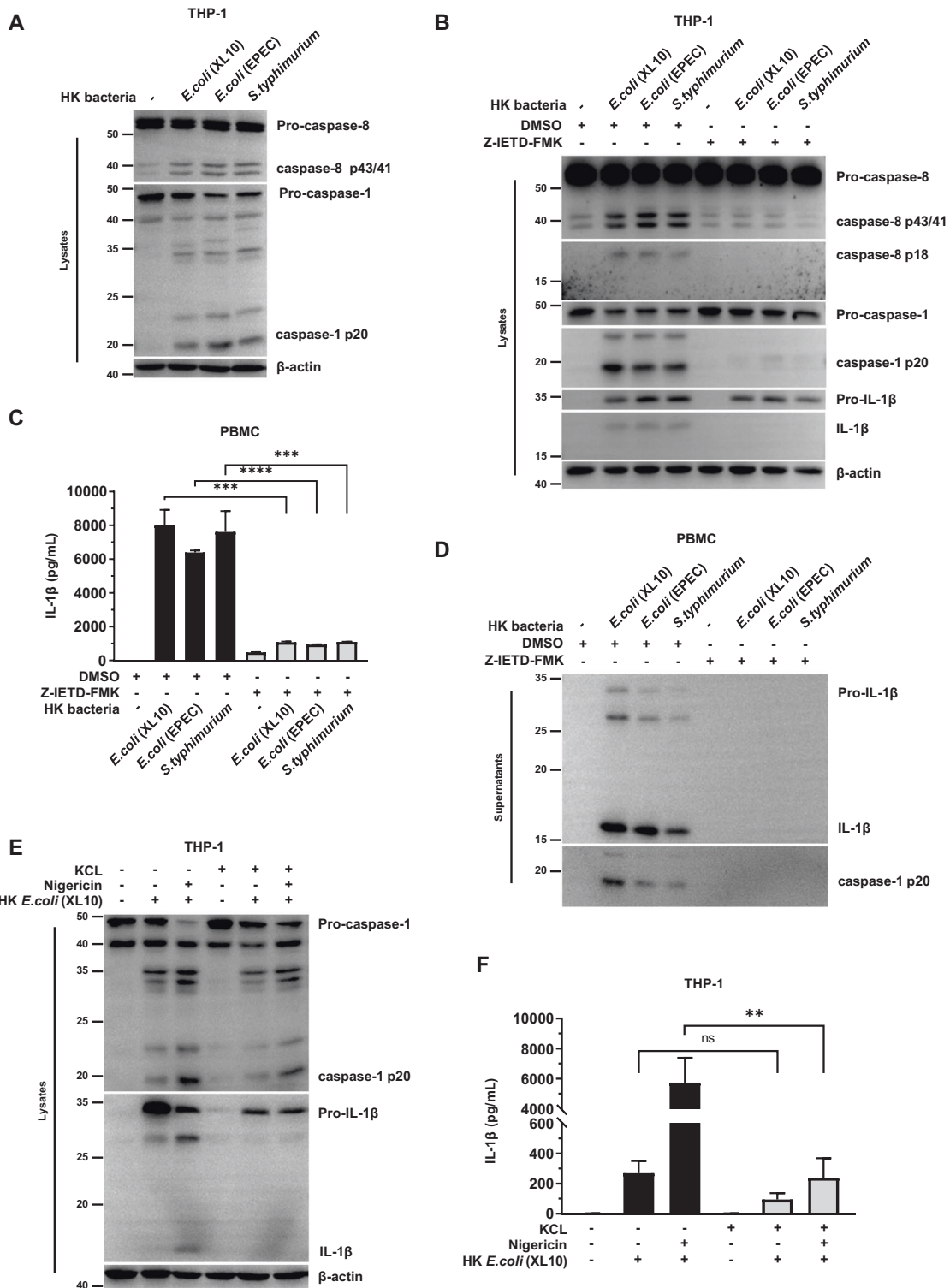
Fig. 2 Heat-killed gram-negative bacteria induce caspase-8 cleavage in human monocytes. **A** THP-1 monocytes were stimulated for 6 h with heat-killed gram-negative bacteria at twice the number of cells. Immunoblots showing caspase-8 and caspase-1 in total cell lysate are representative of one of two experimental repeats. **B** THP-1 monocytes were pretreated for 0.5 h with DMSO or Z-IETD-FMK (25 μM) and stimulated for 6 h with heat-killed gram-negative bacteria at twice the number of cells. Immunoblots showing caspase-8, caspase-1 and IL-1β in total cell lysate are representative of one of two experimental repeats. **C**, **D** PBMCs were pretreated for 0.5 h with DMSO or Z-IETD-FMK (25 μM) and stimulated for 16 h with heat-killed gram-negative bacteria at twice the number of monocytes. **C** The level of IL-1β secreted in the cell culture supernatant is shown as the mean ± SEM based on one of two donors. One-way ANOVA was performed to determine statistical significance. $***p < 0.001$; $****p < 0.0001$. **D** Immunoblots showing IL-1β and caspase-1 in the cell culture supernatant as indicated in **C**. **E**, **F** THP-1 cells were cultured in 30 mM KCl for 10 min and stimulated for 6 h with heat-killed XL10 at twice the number of cells alone or for 1 h with additional nigericin (10 μM). **E** The level of IL-1β secreted in the cell culture supernatant is shown as the mean ± SEM. One-way ANOVA was performed to determine statistical significance. ns, no significant difference; $**p < 0.01$. **F** Immunoblots showing caspase-1 and IL-1β in total cell lysate are representative of one of two experimental repeats

bacteria (Fig. 2F). These results demonstrated that the caspase-8 axis is involved in NLRP3 inflammasome activation induced by heat-killed gram-negative bacteria.

The NLRP3 inflammasome activation induced by heat-killed gram-negative bacteria is intrinsically limited

To better characterize the single-step mild NLRP3 inflammasome activation, we stimulated THP-1 monocytes with heat-killed *E. coli* XL10 in a time course. To this end, seeded THP-1 cells were incubated with heat-killed *E. coli* XL10 for various durations with a 6-hour period (Fig. 3A). The results of this experiment showed that the rate of caspase-1 activation, the degree of GSDMD cleavage and amount of mature IL-1β release into the supernatant reached a plateau at Hour 4 and then remained unchanged until 6 h post-stimulation (Fig. 3A, B); more importantly, the measurement of cleavage rate of caspase-8 followed the same trend (Fig. 3C). Conversely, we stimulated THP-1 cells with heat-killed *E. coli* and added MCC950, an NLRP3 inhibitor, to the culture medium at different timepoints to inhibit the cleavage of caspase-1. The results showed that MCC950 inhibited caspase-1 activation, GSDMD cleavage and IL-1β release at the early stages of these responses but exerted no effect on the late stage of these responses (Supplementary Fig. 4A, B). These results suggested that the rate of the single-step NLRP3 inflammasome activation induced by heat-killed gram-negative bacteria is intrinsically limited.

Many studies have shown that molecules activated by NF-κB play key inhibitory roles in inflammatory responses, such as IKBα, TRAF1 and IRAK-M [24–27]. To explore the mechanisms underlying the negative regulation of the abovementioned alternative inflammasome-associated activation pathways, we pretreated cells with the protein synthesis inhibitor cycloheximide (CHX). Temporal gradient experiments showed that CHX pretreatment resulted in a gradual but sustained time-dependent increase in the cleavage of caspase-1 (Supplementary Fig. 4C, D). In addition, CHX pretreatment significantly enhanced the cleavage rates of caspase-1 and caspase-8, which were accompanied by a significant increase in the cell death rate (Fig. 3D–F). These results suggested that molecules activated after NF-κB activation may play roles in negatively regulating the activity of molecules upstream or in directly regulating caspase-8 activation.

It has been reported that the alternative inflammasome pathway activated by LPS does not lead to cell death, which differs from our results. Next, we used LPS extracted from *E. coli* O111:B4 to characterize cell death mediated through the alternative inflammasome activation pathway. The results showed that a high concentration of LPS induced a small number of cells to die (Supplementary Fig. 5A, B). Compared to the NLRP3 inflammasome activation induced by nigericin, the degrees of caspase-1 activation, GSDMD cleavage and cell death mediated by LPS (2 µg/ml) were extremely low (Supplementary Fig. 5C, D). In addition, CHX pretreatment significantly enhanced LPS-mediated cleavage of caspase-8, caspase-1 and GSDMD, and these results were accompanied by an increase in the cell death rate (Supplementary Fig. 5E–G). These results suggested that alternative inflammasome activation drives cell death in a dose-dependent manner.

The expression of cFLIP is increased in human monocytes after HK-bacteria stimulation

Cell FLICE (FADD-like IL-1β converting enzyme) inhibitory protein (cFLIP) is a major antiapoptotic regulator and resistance factor that inhibits tumor necrosis factor-α (TNF-α), Fas-L and TNF-related apoptosis-inducing ligand (TRAIL)-induced apoptosis [28–30]. In the apoptotic pathway, cFLIP$_L$ and cFLIP$_S$ can bind to FADD and caspase-8 or caspase-10 to form the apoptosis inhibitory complex (AIC). This complex prevents the formation of the death-inducing signaling complex (DISC) and subsequent activation of the caspase cascade [31]. In addition to the apoptotic pathway, cFLIP$_L$ has been reported to exert negative regulatory effects on caspase-8 activity that had been induced by LPS in mouse macrophages [32]. Using

human monocytes, we assessed whether cFLIP negatively regulates the activation of the caspase-8-mediated alternative inflammasome pathway is induced by heat-killed gram-negative bacteria.

The expression of cFLIP isoforms is induced by NF-κB activation [33]. Indeed, stimulating THP-1 monocytic cell activation in a time course experiment showed that the mRNA and protein levels of cFLIP increased significantly within timeframe (Fig. 4A, B). As expected, CHX pretreatment inhibited the expression of cFLIP that was induced by heat-killed gram-negative bacteria, which increased the activation rates of caspase-8 and caspase-1 (Fig. 4C). In addition to THP-1 cells, we measured an increase in cFLIP protein levels in PBMCs in response to heat-killed bacterium-induced stimulation (Fig. 4D).

cFLIP$_S$ negatively regulates the NLRP3 inflammasome activation induced by heat-killed gram-negative bacteria by targeting caspase-8 in human monocytes

Three cFLIP splice variants are expressed as proteins: the 26 kDa short form (cFLIP$_S$), the 24 kDa form (cFLIP$_R$) and the 55 kDa form (cFLIP$_L$). The structure of cFLIP$_S$ is similar to that of cFLIP$_R$, which contains two death effector domains (DEDs) in the N-terminus, but cFLIP$_R$ lacks some of the carboxyl terminal amino acids in cFLIP$_S$. cFLIP$_L$ is longer than cFLIP$_S$ and cFLIP$_R$, and its structure is similar to that of caspase-8, but it does not have a functional caspase domain [31, 34]. This loss of cFLIP catalytic activity is a result of several amino acid substitutions, which is particularly evident when several cysteine residues that are critical for catalytic activity are replaced [35]. To characterize the function of cFLIP variants more specifically, we used lentiviral vectors to generate THP-1 cell lines overexpressing different cFLIP proteins (Supplementary Fig. 6A). We found that only overexpressed cFLIP$_S$, not over-expressed cFLIP$_L$, negatively regulated alternative NLRP3 inflammasome activation in human monocytic cells.

cFLIP binds to caspase-8 through their common death-effector domains (DEDs) to form a heterodimer, inhibiting the catalytic function of caspase-8 [36]. After it was overexpressed in HEK293T cells, cFLIP$_S$ spontaneously interacted with caspase-8 (Fig. 5A). More importantly, in THP-1 cells, overexpressed cFLIP$_S$ inhibited the cleavage of caspase-8 and the activation of caspase-1 that had been triggered in response to heat-killed gram-negative bacterial stimulation (Fig. 5B). Notably, cFLIP$_S$ also inhibited the expression of pro-IL-1β to some extent, suggesting that cFLIP$_S$ negatively regulates NF-κB activation. The weaker activation of caspase-1 and the reduced expression of pro-IL-1β resulted in fewer mature IL-1β molecules being released from cells (Fig. 5B, C). In addition, overexpressed cFLIP$_S$ in THP-1 cells prevented the cell death induced by heat-killed gram-negative bacteria (Fig. 5D, E). Interestingly, the cFLIP$_L$ variant exerted no significant effect on the cleavage of caspase-8 into p43/41, the activation of caspase-1 or the release of mature IL-1β (Supplementary Fig. 6B, C). In addition, PI staining showed that cFLIP$_L$ exerted no significant effect on the cell death induced by heat-killed gram-negative bacteria (Supplementary Fig. 6D, E). In addition, experiments, overexpressed cFLIP$_S$ in THP-1 cells inhibited the cleavage of caspase-8, the activation of caspase-1 and the cell death induced by LPS but exerted no effect on the activation of caspase-1 induced by nigericin or poly(dA:dT) (Supplementary Fig. 7A–E).

cFLIP$_L$ promotes the activation of full-length caspase-8 and its initial autocatalytic processing into caspase-8-p43/41 but inhibits further cleavage to fully active caspase-8-p18, the latter of which is necessary for apoptosis. In contrast, cFLIP$_S$ completely blocks the autoprocessing of full-length caspase-8 into any form [37–40]. This may be the reason that cFLIP$_L$ exerted no apparent effect on the activation of the NLRP3 inflammasome induced by heat-killed gram-negative bacteria in human monocytic cells. Hence, the cleaved form of caspase-8-p43/41 can be considered to play a key role in activating the alternative NLRP3 inflammasome, and cFLIP$_S$ regulate this process by targeting caspase-8.
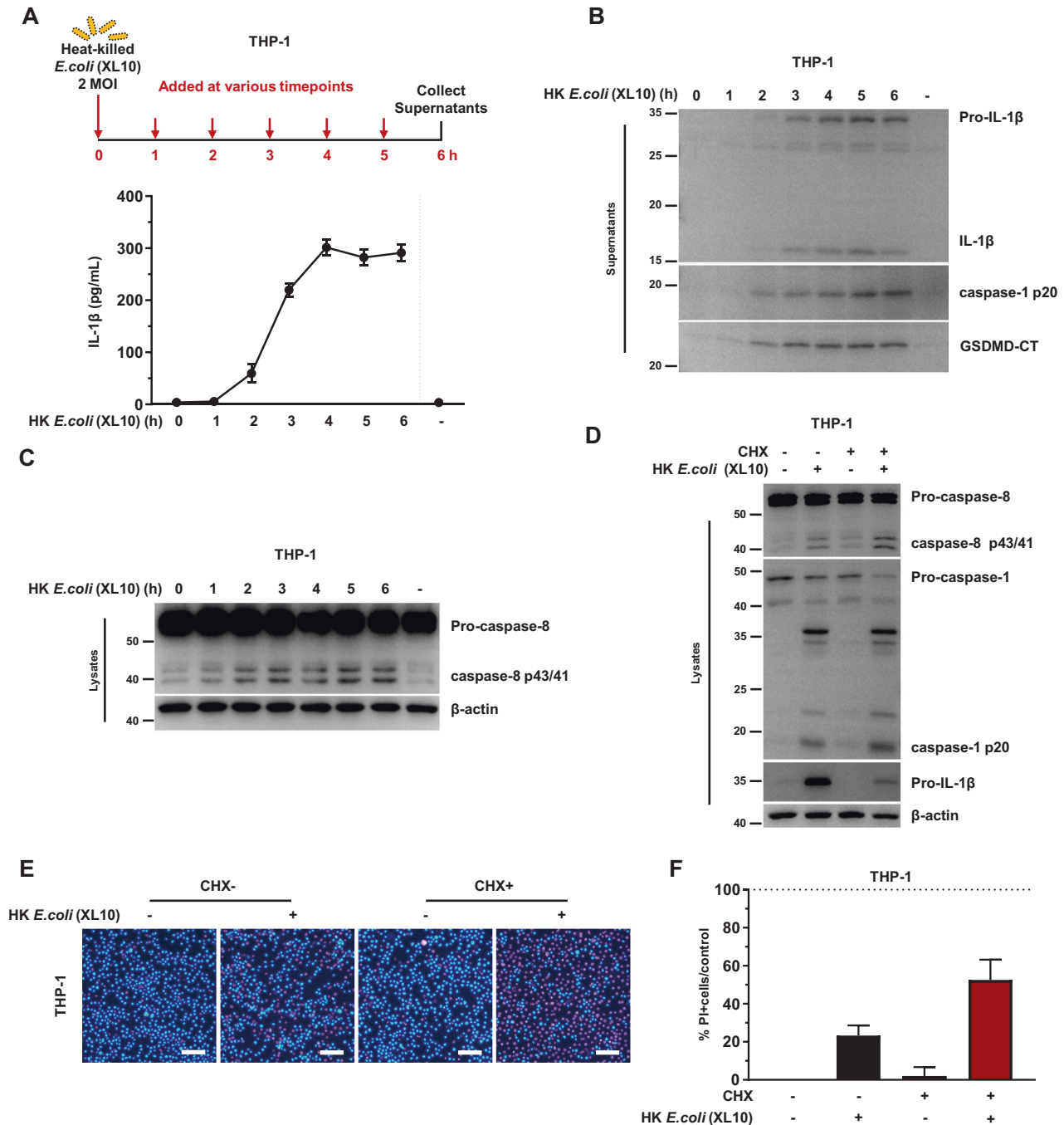
Fig. 3 Alternative NLRP3 inflammasome activation is saturated shortly after initiation. **A, B** THP-1 monocytes were stimulated with heat-killed *E. coli* XL10 in a time course at twice the number of cells. **A** Schematic diagram of the time gradient experiment with heat-killed *E. coli* XL10-stimulated THP-1 monocytes. IL-1β secretion in the cell culture supernatant is shown as the mean ± SEM. **B** Immunoblots showing caspase-1, GSDMD and IL-1β in the cell culture supernatant are representative of one of two experimental repeats. **C** Immunoblot showing caspase-8 in total cell lysate is shown representative of one of two experimental repeats. **D** THP-1 monocytes were left untreated or pretreated for 0.5 h with cycloheximide (CHX, 1 μg/ml) and stimulated for 6 h with heat-killed *E. coli* XL10 at twice the number of cells. Immunoblots showing caspase-8, caspase-1 and IL-1β in total cell lysate are representative of one of two experimental repeats. **E, F** Fluorescence microscopy of THP-1 monocytes after stimulation for 6 h with heat-killed XL10 at twice the number of cells. Cells were left untreated or pretreated for 0.5 h with cycloheximide (1 μg/ml). **E** Cells stained with PI (red) and Hoechst (blue) are representative of one of two experimental repeats. Scale bars denote 100 μm. **F** The PI-positive cells shown in **E** was counted with ImageJ. Error bars show the mean ± SEM

cFLIP knockout enhances the activation of the alternative inflammasome pathway

To characterize the function of cFLIP, we generated *CFLAR*-knockout THP-1 monocytic cell lines using CRISPR–Cas9. The loss of cFLIP significantly increased the cleavage rate of caspase-8 and caspase-1, and these effects were accompanied by an increase in the cell death rate (Fig. 6A–C). Similar results were obtained after LPS stimulation. In addition, experiments, the loss of cFLIP also enhanced alternative inflammasome activation, which led to a higher cell death rate induced by LPS (Supplementary Fig. 8A–C).

The previous results showed that overexpression of cFLIP$_S$, but not cFLIP$_L$, inhibited alternative inflammasome activation more
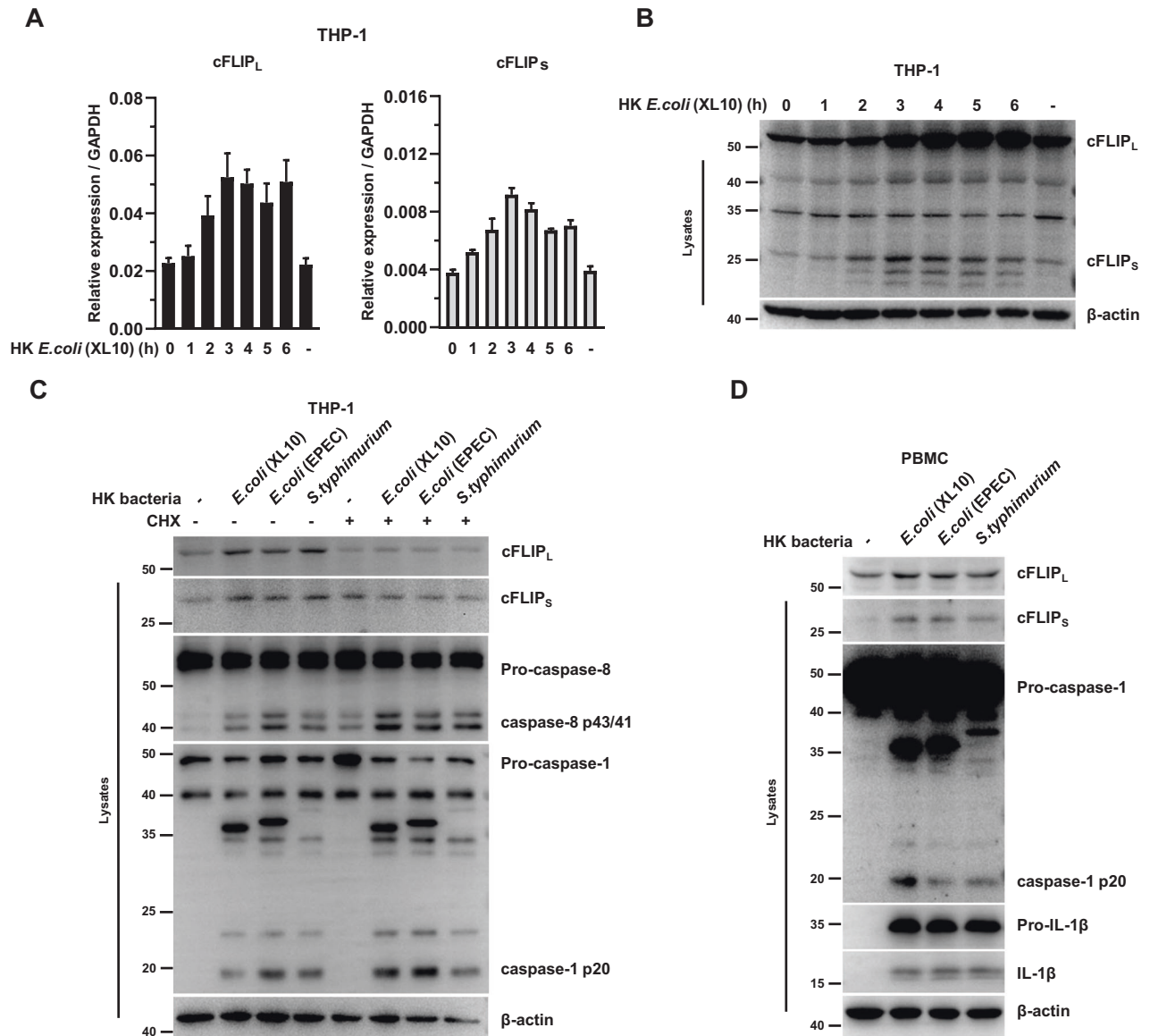
Fig. 4 Expression of cFLIP is induced by heat-killed gram-negative bacteria. **A, B** THP-1 monocytes were stimulated with heat-killed *E. coli* XL10 in a time course at twice the number of cells. **A** Expression of cFLIP was analyzed via qRT–PCR. RNA was isolated from 0.3×10^6 cells. A total of 0.1×10^6 cells per well were seeded, and all treatments were performed in triplicate plates. **B** Immunoblot showing cFLIP in the cell lysate is representative of one of two experimental repeats. **C** THP-1 monocytes were left untreated or pretreated for 0.5 h with cycloheximide (1 μg/ml) and stimulated for 6 h with heat-killed gram-negative bacteria at twice the number of cells. Immunoblots showing cFLIP, caspase-8 and caspase-1 in total cell lysate are representative of one of two experimental repeats. **D** PBMCs were stimulated for 6 h with heat-killed gram-negative bacteria at twice the number of monocytes. Immunoblot showing cFLIP, caspase-1 and IL-1β in the total cell lysate are representative of one of two experimental repeats. The lysate used for the represented blots was generated from the cells obtained from one of two donors

effectively (Fig. 5 and Supplementary Fig. 6). Next, we inserted cFLIP_S back into *CFLAR*-knockout cell lines using lentiviral vectors. The cells were subjected to G418 selection. In *CFLAR*-knockout THP-1 cells, overexpressed cFLIP_S inhibited the excessive cleavage of caspase-8 and the activation of caspase-1, accompanied by a decrease in the cell death rate (Fig. 6D–F). In addition, overexpressed cFLIP_S inhibited the excessive cleavage of caspase-8 and caspase-1 induced by LPS, which led to a reduced cell death rate(Supplementary Fig. 8D–F).

It has been reported that the alternative inflammasome activation pathway does not lead to cell death. We obtained the similar results when low concentrations of LPS were used. However, our results suggested that cells died in response to stronger stimuli, such as heat-killed bacteria or high

concentrations of LPS. Inflammasome activation at low concentrations of a stimulant may be not sufficient to induce pyroptosis. The loss of cFLIP increased inflammasome activation rate, which led to more cells dying.

TAK1 is a master regulator of caspase-8, cFLIP_S and NLRP3 in human monocytes

Transforming growth factor β-activated kinase 1 (TAK1) is a key regulator of innate immunity related to caspase-8 [41]. Studies have shown that loss of TAK1 catalytic activity led to the excessive activation of caspase-8 in mouse macrophages. The activation of caspase-8 cleaved caspase-3 and caspase-7 to initiate apoptosis [42]. Simultaneously, caspase-8 cleaved GSDMD in mouse macrophages to induce pyroptosis. However, TAK1 inhibition and
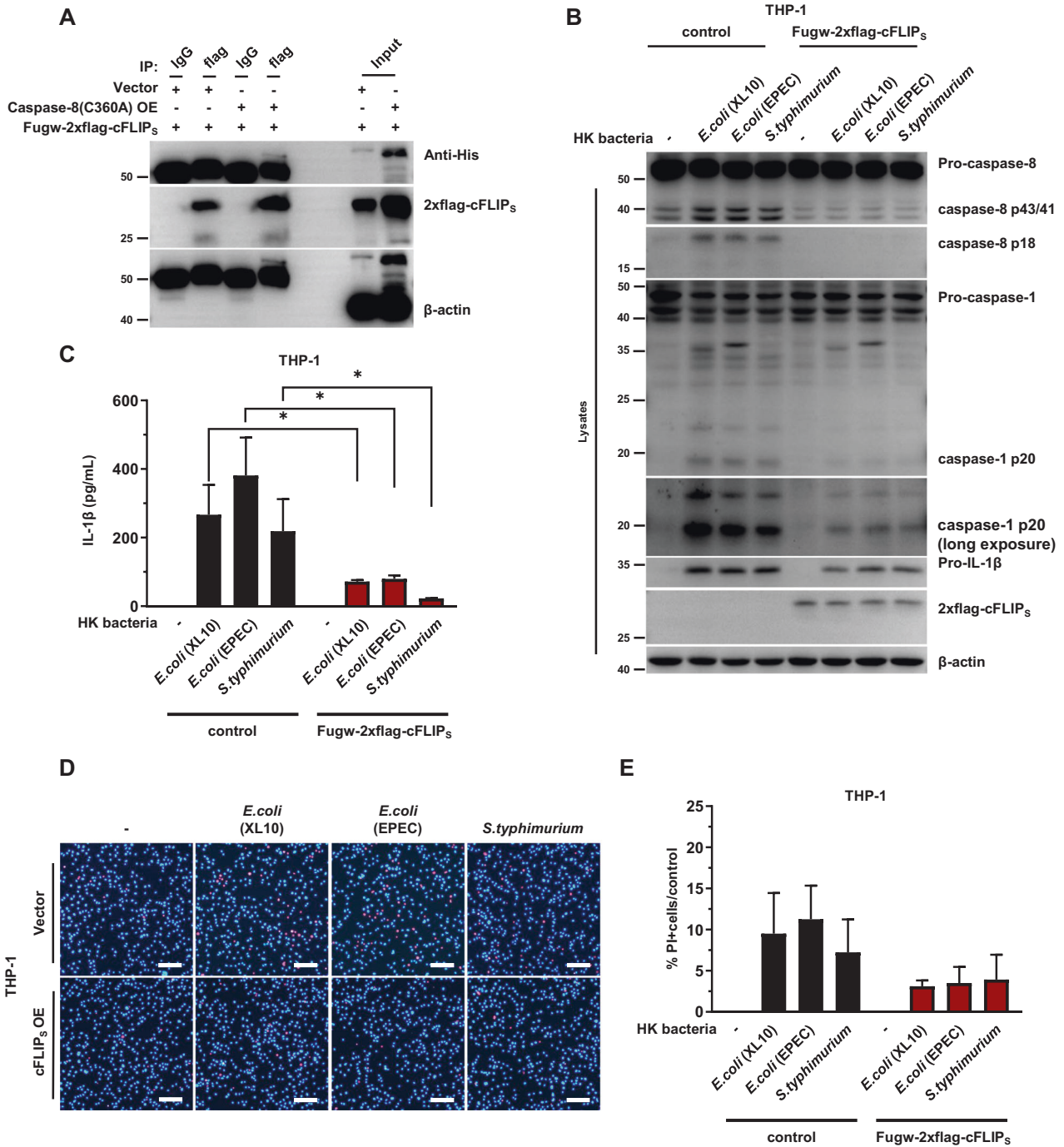
Fig. 5 cFLIP$_S$ negatively regulates NLRP3 inflammasome activation by inhibiting caspase-8 cleavage. **A** The interaction between cFLIP$_S$ and caspase-8 was verified in 293T cells. 293T cells were transfected with 400 ng of fugw-2xflag-cFLIP$_S$ and 200 ng of PCDN4-caspase-8(C360A)-His plasmids in 24-well plates. Immunoblots showing cFLIP and His-tag are representative of one of two experimental repeats. **B**, **C** Control and OE-fugw-2xflag-cFLIP$_S$ THP-1 monocytes were stimulated for 6 h with heat-killed gram-negative bacteria at twice the number of cells. **B** Immunoblots showing caspase-8, caspase-1, IL-1β and cFLIP$_S$ in total cell lysate are representative of one of three experimental repeats. **C** The level of IL-1β secreted in the cell culture supernatant is shown as the mean ± SEM. One-way ANOVA was performed to determine statistical significance. *$p < 0.05$. **D**, **E** Fluorescence microscopy of THP-1 monocytes after stimulation for 6 h with heat-killed gram-negative bacteria at twice the number of cells. **D** Cells stained with PI (red) and Hoechst (blue) are representative of one of two experimental repeats. Scale bars denote 100 μm. **E** The number of PI-positive cells shown in **D** was counted by ImageJ. Error bars show the mean ± SEM

deficiency in human monocytes did not cause spontaneous cell death [43, 44]. Hence, we performed experiments to reassess the need for TAK1 and caspase-8 activation induced by heat-killed gram-negative bacteria in human monocytes. Raptinal can initiate intrinsic pathway-dependent apoptosis [45]. In contrast to its promoting effect on apoptosis in murine macrophages, the

cleavage of full-length caspase-8 induced by HK bacteria did not lead to caspase-3 activation in human monocytes (Fig. 7A).

Notably, we found that the TAK1 kinase inhibitor 5Z-7-oxo inhibited the cleavage of caspase-8 and caspase-1 (Fig. 7B) [46]. To characterize the effect of TAK1 ablation, we generated *MAP3K7*-knockout THP-1 monocytic cells using CRISPR–Cas9. The loss of
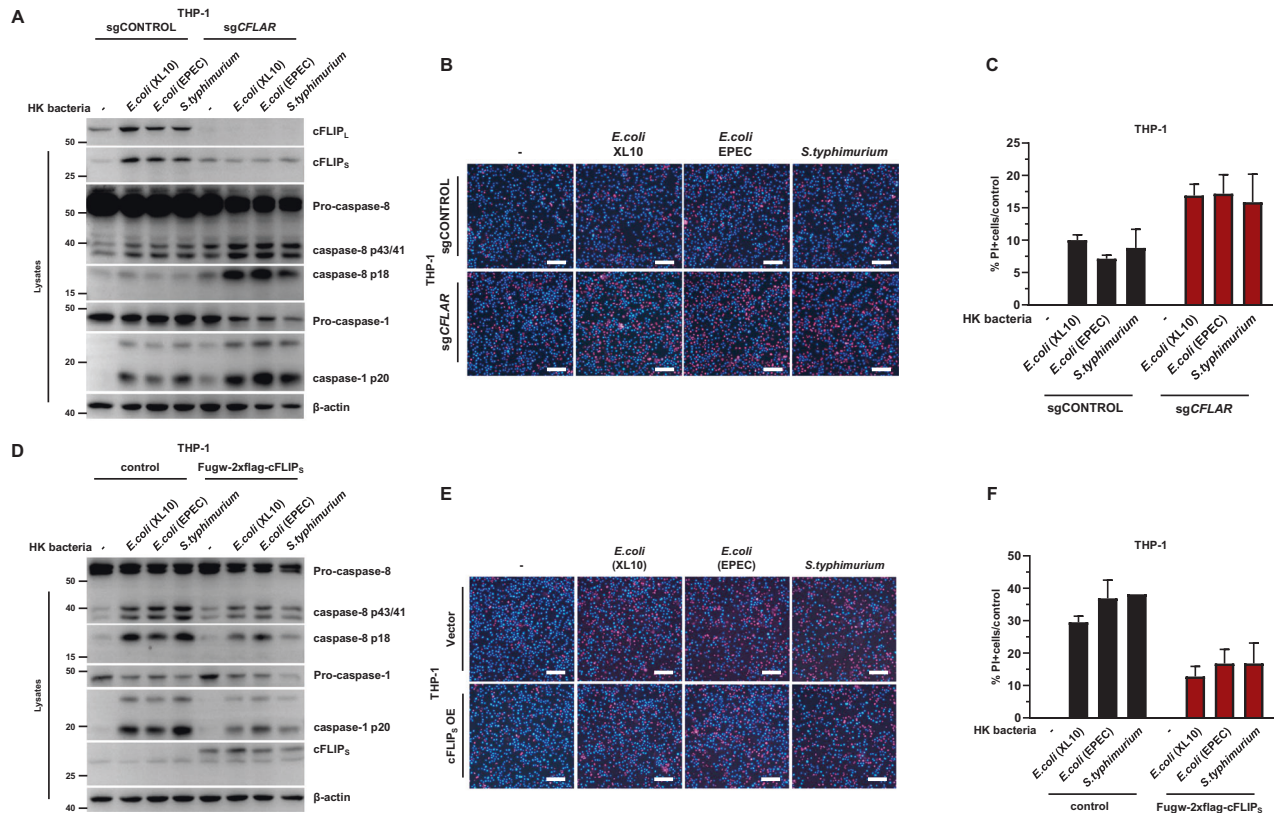
Fig. 6 Ablation of cFLIP enhances NLRP3 inflammasome activation. **A–C** Control and *CFLAR*-KO THP-1 monocytes were stimulated for 6 h with heat-killed gram-negative bacteria at twice the number of cells. **A** Immunoblots showing cFLIP, caspase-8 and caspase-1 in total cell lysate are representative of one of two experimental repeats. **B** Cells stained with PI (red) and Hoechst (blue) are representative of one of two experimental repeats. Scale bars denote 100 μm. **C** The number of PI-positive cells shown in **B** was counted by ImageJ. Error bars show the mean ± SEM. **D–F** Control and OE-fugw-2xflag-cFLIP$_S$ *CFLAR* KO THP-1 monocytes were stimulated for 6 h with heat-killed gram-negative bacteria at twice the number of cells. **D** Immunoblots showing caspase-8, caspase-1 and cFLIP$_S$ in total cell lysate are representative of one of two experimental repeats. **E** Cells stained with PI (red) and Hoechst (blue) are representative of one of two experimental repeats. Scale bars denote 100 μm. **F** The number of PI-positive cells shown in **E** was counted by ImageJ. Error bars show the mean ± SEM

TAK1 did not lead to apoptosis induced by heat-killed gram-negative bacteria but significantly inhibited downstream caspase-8 and caspase-1 activation (Fig. 7C, Supplementary Fig. 9A, B). In further experiments, Z-IETD-FMK inhibited the activation of caspase-8 but exerted no effect on the phosphorylation of TAK1 (Fig. 7D), suggesting that caspase-8 cleavage occurs downstream of TAK1 kinase activation. However, TAK1 ablation exerted no effect on necroptosis mediated by TBZ (TNF-α + BV6 + Z-VAD-FMK) (Supplementary Fig. 9C, D). In addition, 5Z-7-oxo inhibited the expression of the cFLIP isoforms (Fig. 7E), which was consistent with findings in a previous report [32]. These results demonstrated that TAK1 plays different roles in caspase-8 activation in human monocytes, wherein TAK1 acts upstream of caspase-8 to activate the alternative NLRP3 inflammasome pathway.

TAK1 plays a key role in proinflammatory signaling through the activation of NF-κB downstream of TLR [47]. In addition to its function in NF-κB signaling, TAK1 inhibition has been shown to cause excessive activation of caspase-8 in mouse macrophages. In the present study on human monocytes, we found that TAK1 was a master regulator of alternative NLRP3 inflammasome activation and cFLIP expression. Moreover, TAK1 knockout prevented NLRP3 inflammasome activation, and inhibition of TAK1 did not lead to cell death in monocytes treated with heat-killed gram-negative bacteria. Our results thus suggest that TAK1 is functionally diverse in different cells and species.

Finally, we examined the effects of other molecules in the NF-κB pathway on the activation of the NLRP3 inflammasome. Notably,

we found that cFLIP expression was inhibited by an IKK-β inhibitor (TPCA1) or NF-κB inhibitor (BAY 11-7082) (Supplementary Fig. 10a). These results demonstrated that the expression of cFLIP isoforms was mediated by NF-κB activation. However, TPCA1 pretreatment inhibited the activation of caspase-1 induced by heat-killed XL10 (Supplementary Fig. 10B) [48]. To further characterize the effect of P65, we generated *RELA*-knockout THP-1 monocytic cells using CRISPR–Cas9. The results showed that the loss of P65 enhanced the activation of caspase-1, which led to more cells dying (Supplementary Fig. 10D, E).

DISCUSSION
The current understanding of an alternative pathway of inflammasome activation induced by LPS suggests that cell death is undetectable and is mediated independent of K$^+$ efflux in human monocytes [13]. Here, we describe that noninvasive heat-killed gram-negative bacteria, as more physiologically relevant stimuli, activated the NLRP3 inflammasome in human monocytes. As previously shown, alternative NLRP3 inflammasome activation induced by heat-killed gram-negative bacteria was dependent on caspase-8 and independent of K$^+$ efflux. Notably, mature IL-1β release resulting from activation of the alternative NLRP3 inflammasome pathway was finished shortly after it was initiated. This saturation effect was inhibited by CHX and accompanied by an increase in the cell death rate. To this end, we demonstrated that the expression of cFLIP$_S$ induced by HK bacteria inhibited further activation of NLRP3; thus, cFLIP$_S$ is crucial for the balance between host defense and cell
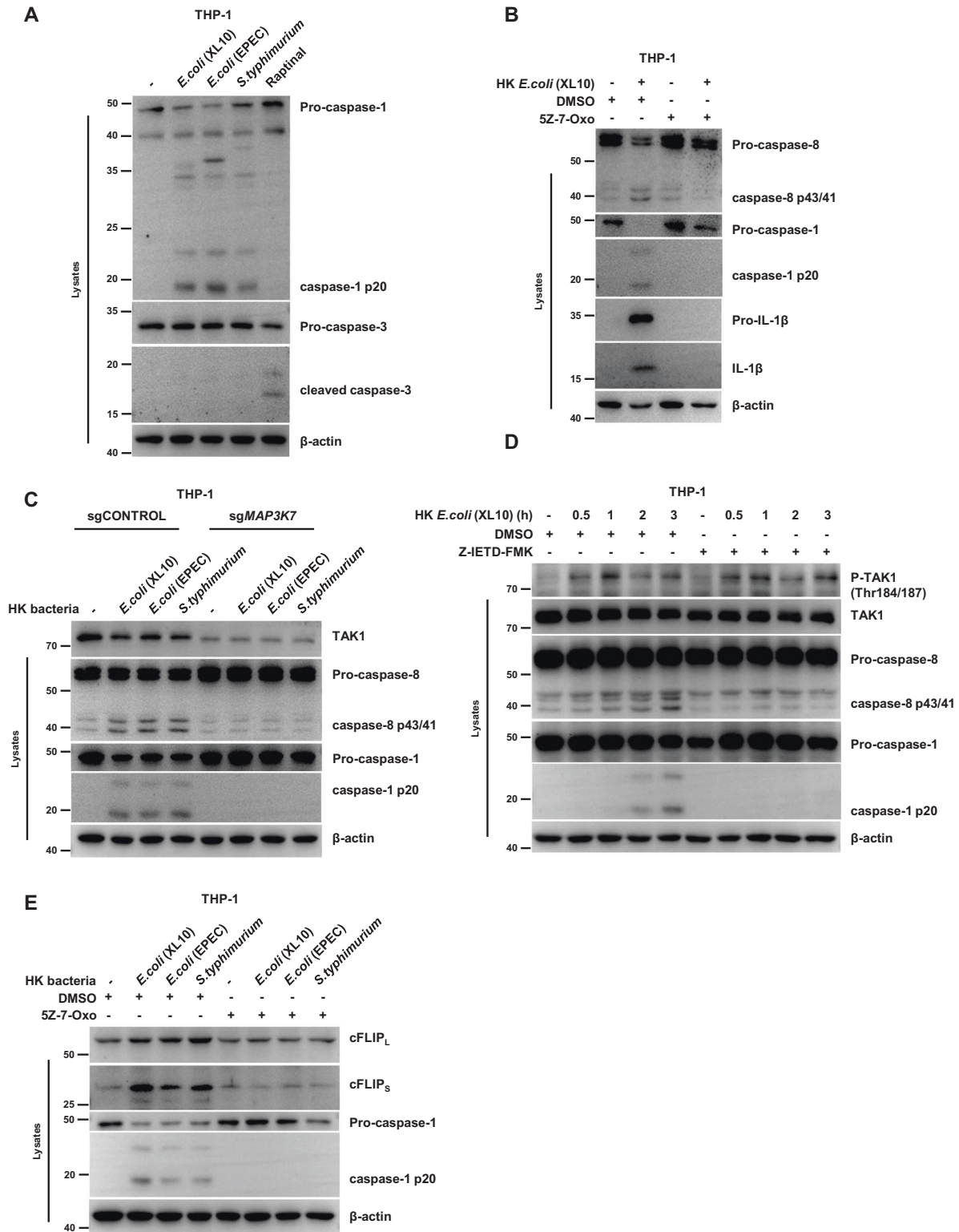
Fig. 7 TAK1 is involved in alternative NLRP3 inflammasome pathway activation. **A** THP-1 monocytes were stimulated for 6 h with heat-killed gram-negative bacteria at twice the number of cells or for 1 h with raptinal (1 μg/ml). Immunoblots showing caspase-1 and caspase-3 in total cell lysate are representative of one of two experimental repeats. **B** THP-1 monocytes were pretreated for 0.5 h with DMSO or 5Z-7-oxozeaenol (1 μM) and stimulated for 6 h with heat-killed *E. coli* XL10 at twice the number of cells. Immunoblots showing caspase-8, caspase-1 and IL-1β in total cell lysate are representative of one of two experimental repeats. **C** Control and *MAP3K7* KO THP-1 monocytes were stimulated for 6 h with heat-killed gram-negative bacteria at twice the number of cells. Immunoblots showing TAK1, caspase-8 and caspase-1 in total cell lysate are representative of one of two experimental repeats. **D** THP-1 monocytes were pretreated for 0.5 h with DMSO or Z-IETD-FMK (25 μM) and stimulated at a specific time point with heat-killed *E. coli* XL10 at twice the number of cells. Immunoblots showing P-TAK1, caspase-8 and caspase-1 in total cell lysate are representative of one of two experimental repeats. **E** THP-1 monocytes were pretreated for 0.5 h with DMSO or 5Z-7-oxozeaenol (1 μM) and stimulated for 6 h with heat-killed *E. coli* XL10 at twice the number of cells. Immunoblots showing cFLIP and caspase-1 in total cell lysate are representative of one of two experimental repeats

survival. Moreover, TAK1 was found to be involved in alternative inflammasome pathway activation and exhibited functions that differed from those of mouse macrophages [42].

As the initial caspase in the extrinsic apoptosis pathway, caspase-8 can be activated in various ways and mediates multiple types of cell death; it also inhibits necroptosis mediated by RIPK3 and MLKL by cleaving RIPK1 [49–52]. As a molecular switch for apoptosis, necroptosis and pyroptosis, caspase-8 can also be activated by LPS in murine macrophages after TAK1 activity is inhibited, which leads to the activation of caspase-3 and GSDMD cleavage. GSDMD pore formation triggers NLRP3 inflammasome activation. [42, 43]. Notably, in murine macrophages, inhibition of TAK1 led to the excessive activation of caspase-8, which was due to the attenuated expression of cFLIP [32]. However, in human monocytes, the caspase-8 cleavage-mediated activation of the alternative inflammasome pathway, which was independent of K^+ efflux, did not lead to caspase-3 activation. Moreover, our results suggested that insufficient cleavage of caspase-8 to p43/41 plays a key role in activating the alternative NLRP3 inflammasome pathway because $cFLIP_L$ prevented the full cleavage of caspase-8 into p18 and exerted no clear effect on its cleavage into the p43/41 form, thus exerting no effect on the activation of the NLRP3 inflammasome. In contrast, $cFLIP_S$ completely blocked the cleavage of caspase-8 (preventing the generation of both p43/41 and p18), thus inhibiting the activation of the NLRP3 inflammasome. Moreover, overexpressed $cFLIP_S$, but not over-expressed $cFLIP_L$, inhibited the expression of pro-IL-1β to some extent, which may have been a result of the inhibition of caspase-8 cleavage into p43/41, which may have also inhibited NF-kB activation, as previously reported [53, 54].

TAK1 is activated by cytokine receptors and bacterial ligands, leading to a cellular response through signal transduction [21]. After activation, TAK1 mediates the activation of downstream Iκb kinase (IKK), thereby promoting the entry of NF-κB dimers into the nucleus to drive the expression of target genes. Many target genes induced by the NF-κB pathway inhibit apoptosis, promote cell proliferation and stimulate inflammatory responses [47, 55, 56]. In murine macrophages, cFLIP expression is diminished after TAK1 activity is inhibited, which leads to the excessive activation of caspase-8 and cell death [32]. Although cFLIP expression in human monocytes is also mediated by TAK1, the inhibition of TAK1 does not result in increased caspase-8 cleavage. TAK1 mediates the activation of the NF-κB pathway and is also required for caspase-8 cleavage induced by heat-killed gram-negative bacteria. Accordingly, TAK1 inhibition did not promote cell death with or without HK bacterial stimulation. Our results therefore provide evidence for further understanding the interplay between NF-κB and alternative inflammasome activation pathways.

An appropriate degree of immune response, such as physiological inflammation, is necessary for a host to respond to microbial infections. The negative regulatory mechanism of the inflammatory response can prevent irreversible damage to tissues and the whole body [17, 57]. Our results hereby demonstrate that $cFLIP_S$ negatively regulates alternative inflammasome activation in human monocytes, which prevents cell death caused by otherwise sustained NLRP3 inflammasome activation. In addition, appropriate IL-1β release during cell survival is necessary for the body to respond to pathogen infection. In this process, TAK1 not only mediates the expression of downstream cFLIP but is also involved in the cleavage of caspase-8. The results of this study provide a new understanding of an alternative inflammasome pathway that leads to a minimal death rate of human monocytes.

REFERENCES

1. Janeway CA Jr. Approaching the asymptote? Evolution and revolution in immunology. Cold Spring Harb Symp Quant Biol. 1989;54:1–13.
2. Medzhitov R. Approaching the asymptote: 20 years later. Immunity. 2009;30:766–75.
3. Fernandes-Alnemri T, Wu J, Yu JW, Datta P, Miller B, Jankowski W, et al. The pyroptosome: a supramolecular assembly of ASC dimers mediating inflammatory cell death via caspase-1 activation. Cell Death Differ. 2007;14:1590–604.
4. Thornberry NA, Bull HG, Calaycay JR, Chapman KT, Howard AD, Kostura MJ, et al. A novel heterodimeric cysteine protease is required for interleukin-1-beta processing in monocytes. Nature. 1992;356:768–74.
5. Gu Y, Kuida K, Tsutsui H, Ku G, Hsiao K, Fleming MA, et al. Activation of interferon-gamma inducing factor mediated by interleukin-1beta converting enzyme. Science. 1997;275:206–9.
6. Shi J, Zhao Y, Wang K, Shi X, Wang Y, Huang H, et al. Cleavage of GSDMD by inflammatory caspases determines pyroptotic cell death. Nature. 2015;526:660–5.
7. Xia S, Zhang Z, Magupalli VG, Pablo JL, Dong Y, Vora SM, et al. Gasdermin D pore structure reveals preferential release of mature interleukin-1. Nature. 2021;593:607–11.
8. Yang J, Liu Z, Xiao TS. Post-translational regulation of inflammasomes. Cell Mol Immunol. 2017;14:65–79.
9. Shi J, Zhao Y, Wang Y, Gao W, Ding J, Li P, et al. Inflammatory caspases are innate immune receptors for intracellular LPS. Nature. 2014;514:187–92.
10. Kayagaki N, Warming S, Lamkanfi M, Vande Walle L, Louie S, Dong J, et al. Non-canonical inflammasome activation targets caspase-11. Nature. 2011;479:117–21.
11. Kayagaki N, Stowe IB, Lee BL, O'Rourke K, Anderson K, Warming S, et al. Caspase-11 cleaves gasdermin D for non-canonical inflammasome signalling. Nature. 2015;526:666–71.
12. Martin-Sanchez F, Diamond C, Zeitler M, Gomez AI, Baroja-Mazo A, Bagnall J, et al. Inflammasome-dependent IL-1 beta release depends upon membrane permeabilisation. Cell Death Differ. 2016;23:1219–31.
13. Gaidt MM, Ebert TS, Chauhan D, Schmidt T, Schmid-Burgk JL, Rapino F, et al. Human monocytes engage an alternative inflammasome pathway. Immunity. 2016;44:833–46.
14. Zewinger S, Jochen R, Jankowski V, Hahm E, Schunk S, Schmit D, et al. Apolipoprotein C3 induces systemic inflammation and organ damage in Ckd by alternative inflammasome activation via a novel pathway. Nephrol Dial Transpl. 2019;34:gfz096.FO084.
15. Gaidt MM, Hornung V. Alternative inflammasome activation enables IL-1β release from living cells. Curr Opin Immunol. 2017;44:7–13.
16. Morgado FN, de Carvalho LMV, Leite-Silva J, Seba AJ, Pimentel MIF, Fagundes A, et al. Unbalanced inflammatory reaction could increase tissue destruction and worsen skin infectious diseases - a comparative study of leishmaniasis and sporotrichosis. Sci Rep. 2018;8:2898.
17. Anderton H, Wicks IP, Silke J. Cell death in chronic inflammation: breaking the cycle to treat rheumatic disease. Nat Rev Rheumatol. 2020;16:496–513.
18. Headland SE, Norling LV. The resolution of inflammation: principles and challenges. Semin Immunol. 2015;27:149–60.
19. Sugimoto MA, Sousa LP, Pinho V, Perretti M, Teixeira MM. Resolution of inflammation: what controls its onset? Front Immunol. 2016;7:160.
20. Afonina IS, Zhong Z, Karin M, Beyaert R. Limiting inflammation-the negative regulation of NF-kappaB and the NLRP3 inflammasome. Nat Immunol. 2017;18:861–9.
21. Yu S, Green J, Wellens R, Lopez-Castejon G, Brough D. Bafilomycin A1 enhances NLRP3 inflammasome activation in human monocytes independent of lysosomal acidification. FEBS J. 2021;288:3186–96
22. Munoz-Planillo R, Kuffa P, Martinez-Colon G, Smith BL, Rajendiran TM, Nunez G. K + efflux is the common trigger of NLRP3 inflammasome activation by bacterial toxins and particulate matter. Immunity. 2013;38:1142–53.
23. Ruhl S, Broz P. Caspase-11 activates a canonical NLRP3 inflammasome by promoting K+ efflux. Eur J Immunol. 2015;45:2927–36.
24. Peng B, Ling J, Lee AJ, Wang Z, Chang Z, Jin W, et al. Defective feedback regulation of NF-kappaB underlies Sjogren's syndrome in mice with mutated kappaB enhancers of the IkappaBalpha promoter. Proc Natl Acad Sci USA. 2010;107:15193–8.
25. Alves BN, Tsui R, Almaden J, Shokhirev MN, Davis-Turak J, Fujimoto J, et al. I kappa B epsilon is a key regulator of B cell expansion by providing negative feedback on cRel and RelA in a stimulus-specific manner. J Immunol. 2014;192:3121–32.
26. Abdul-Sater AA, Edilova MI, Clouthier DL, Mbanwi A, Kremmer E, Watts TH. The signaling adaptor TRAF1 negatively regulates Toll-like receptor signaling and this underlies its role in rheumatic disease. Nat Immunol. 2017;18:26–35.
27. Kobayashi K, Hernandez LD, Galan JE, Janeway CA, Medzhitov R, Flavell RA. IRAK-M is a negative regulator of toll-like receptor signaling. Cell. 2002;110:191–202.
28. Panayotova-Dimitrova D, Feoktistova M, Ploesser M, Kellert B, Hupe M, Horn S, et al. cFLIP regulates skin homeostasis and protects against TNF-induced keratinocyte apoptosis. Cell Rep. 2013;5:397–408.
29. Thome M, Schneider P, Hofmann K, Fickenscher H, Meinl E, Neipel F, et al. Viral FLICE-inhibitory proteins (FLIPs) prevent apoptosis induced by death receptors. Nature. 1997;386:517–21.

30. Geserick P, Drewniok C, Hupe M, Haas TL, Diessenbacher P, Sprick MR, et al. Suppression of cFLIP is sufficient to sensitize human melanoma cells to TRAIL- and CD95L-mediated apoptosis. Oncogene. 2008;27:3211–20.

31. Budd RC, Yeh WC, Tschopp J. cFLIP regulation of lymphocyte activation and development. Nat Rev Immunol. 2006;6:196–204.

32. Muendlein HI, Jetton D, Connolly WM, Eidell KP, Magri Z, Smirnova I, et al. cFLIP(L) protects macrophages from LPS-induced pyroptosis via inhibition of complex II formation. Science. 2020;367:1379–84.

33. Micheau O, Lens S, Gaide O, Alevizopoulos K, Tschopp J. NF-kappaB signals induce the expression of c-FLIP. Mol Cell Biol. 2001;21:5299–305.

34. Safa AR, Pollok KE. Targeting the anti-apoptotic protein c-FLIP for cancer therapy. Cancers. 2011;3:1639–71.

35. Irmler M, Thome M, Hahne M, Schneider P, Hofmann K, Steiner V, et al. Inhibition of death receptor signals by cellular FLIP. Nature. 1997;388:190–5.

36. Hu SM, Vincenz C, Buller M, Dixit VM. A novel family of viral death effector domain-containing molecules that inhibit both CD-95- and tumor necrosis factor receptor-1-induced apoptosis. J Biol Chem. 1997;272:9621–4.

37. Krueger A, Schmitz I, Baumann S, Krammer PH, Kirchhoff S. Cellular FLICE-inhibitory protein splice variants inhibit different steps of caspase-8 activation at the CD95 death-inducing signaling complex. J Biol Chem. 2001;276:20633–40.

38. Chang DW, Xing Z, Pan Y, Algeciras-Schimnich A, Barnhart BC, Yaish-Ohad S, et al. c-FLIPL is a dual function regulator for caspase-8 activation and CD95-mediated apoptosis. Embo J. 2002;21:3704–14.

39. Micheau O, Tschopp J. Induction of TNF receptor I-mediated apoptosis via two sequential signaling complexes. Cell. 2003;114:181–90.

40. Kataoka T, Tschopp J. N-terminal fragment of c-FLIP(L) processed by caspase 8 specifically interacts with TRAF2 and induces activation of the NF-kappaB signaling pathway. Mol Cell Biol. 2004;24:2627–36.

41. Ajibade AA, Wang HY, Wang RF. Cell type-specific function of TAK1 in innate immune signaling. Trends Immunol. 2013;34:307–16.

42. Orning P, Weng D, Starheim K, Ratner D, Best Z, Lee B, et al. Pathogen blockade of TAK1 triggers caspase-8-dependent cleavage of gasdermin D and cell death. Science. 2018;362:1064–9.

43. Sarhan J, Liu BC, Muendlein HI, Li P, Nilson R, Tang AY, et al. Caspase-8 induces cleavage of gasdermin D to elicit pyroptosis during Yersinia infection. Proc Natl Acad Sci USA. 2018;115:E10888–E97.

44. Schmacke NA, O'Duill F, Gaidt MM, Szymanska I, Kamper JM, Schmid-Burgk JL, et al. IKKbeta primes inflammasome formation by recruiting NLRP3 to the trans-Golgi network. Immunity. 2022;55:2271–84.e7.

45. Palchaudhuri R, Lambrecht MJ, Botham RC, Partlow KC, van Ham TJ, Putt KS, et al. A Small molecule that induces intrinsic pathway apoptosis with unparalleled speed. Cell Rep. 2015;13:2027–36.

46. Ninomiya-Tsuji J, Kajino T, Ono K, Ohtomo T, Matsumoto M, Shiina M, et al. A resorcylic acid lactone, 5Z-7-oxozeaenol, prevents inflammation by inhibiting the catalytic activity of TAK1 MAPK kinase kinase. J Biol Chem. 2003;278:18485–90.

47. Takaesu G, Surabhi RM, Park KJ, Ninomiya-Tsuji J, Matsumoto K, Gaynor RB. TAK1 is critical for I kappa B kinase-mediated activation of the NF-kappa B pathway. J Mol Biol. 2003;326:105–15.

48. Unterreiner A, Rubert J, Kauffmann M, Fruhauf A, Heiser D, Erbel P, et al. Pharmacological inhibition of IKKbeta dampens NLRP3 inflammasome activation after priming in the human myeloid cell line THP-1. Biochem Biophys Res Commun. 2021;545:177–82.

49. Boldin MP, Goncharov TM, Goltsev YV, Wallach D. Involvement of MACH, a novel MORT1/FADD-interacting protease, in Fas/APO-1- and TNF receptor-induced cell death. Cell 1996;85:803–15.

50. Varfolomeev EE, Schuchmann M, Luria V, Chiannilkulchai N, Beckmann JS, Mett IL, et al. Targeted disruption of the mouse Caspase 8 gene ablates cell death induction by the TNF receptors, Fas/Apo1, and DR3 and is lethal prenatally. Immunity. 1998;9:267–76.

51. Kaiser WJ, Upton JW, Long AB, Livingston-Rosanoff D, Daley-Bauer LP, Hakem R, et al. RIP3 mediates the embryonic lethality of caspase-8-deficient mice. Nature. 2011;471:368.

52. Alvarez-Diaz S, Dillon CP, Lalaoui N, Tanzer MC, Rodriguez DA, Lin A, et al. The pseudokinase MLKL and the kinase RIPK3 have distinct roles in autoimmune disease caused by loss of death-receptor-induced apoptosis. Immunity. 2016;45:513–26.

53. Su H, Bidere N, Zheng LX, Cubre A, Sakai K, Dale J, et al. Requirement for caspase-8 in NF-kappa B activation by antigen receptor. Science. 2005;307:1465–8.

54. Bidere N, Snow AL, Sakai K, Zheng LX, Lenardo MJ. Caspase-8 regulation by direct interaction with TRAF6 in T cell receptor-induced NF-kappa B activation. Curr Biol. 2006;16:1666–71.

55. Hayden MS, Ghosh S. Shared principles in NF-kappaB signaling. Cell. 2008;132:344–62.

56. Liu T, Zhang L, Joo D, Sun SC. NF-kappaB signaling in inflammation. Signal Transduct Target Ther. 2017;2:17023. -

57. Gao HM, Hong JS. Why neurodegenerative diseases are progressive: uncontrolled inflammation drives disease progression. Trends Immunol. 2008;29:357–65.

ACKNOWLEDGEMENTS

AUTHOR CONTRIBUTIONS

SY and GM conceived the project. YG conducted most experiments; SY, MC, XW, LP, and BW helped with experiments and prepared critical reagents; YG, SY, and GM analyzed the data and wrote the manuscript.

COMPETING INTERESTS

The authors declare no competing interests.

ADDITIONAL INFORMATION

Supplementary information The online version contains supplementary material available at https://doi.org/10.1038/s41423-023-01077-y.

Correspondence and requests for materials should be addressed to Bin Wei or Guangxun Meng.

Reprints and permission information is available at http://www.nature.com/reprints